

Supporting Information

Dynamic Role of the Intramolecular Hydrogen Bonding in Nonadiabatic Chemistry Revealed in the UV Photodissociation Reactions of 2-Fluorothiophenol and 2-Chlorothiophenol

*Songhee Han^{‡†}, Hyun Sik You[‡], So-Yeon Kim and Sang Kyu Kim**

Department of Chemistry, KAIST, Daejeon 305-701, Republic of Korea

[†]Present address: Max Born Institute for Nonlinear Optics and Short Pulse Spectroscopy in Berlin Research Association, Max-Born-Str. 2 A 12489, Berlin

*Author to whom correspondence should be addressed.



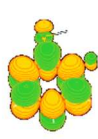
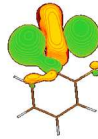
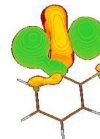
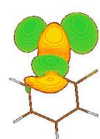

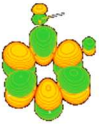
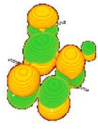


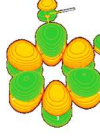
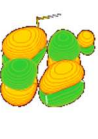
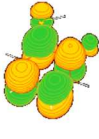
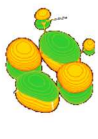


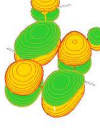

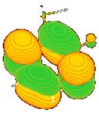

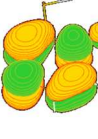
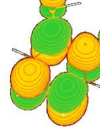
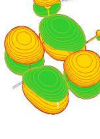
E-mail: sangkyukim@kaist.ac.kr Tel: (+)82-42-350-2843

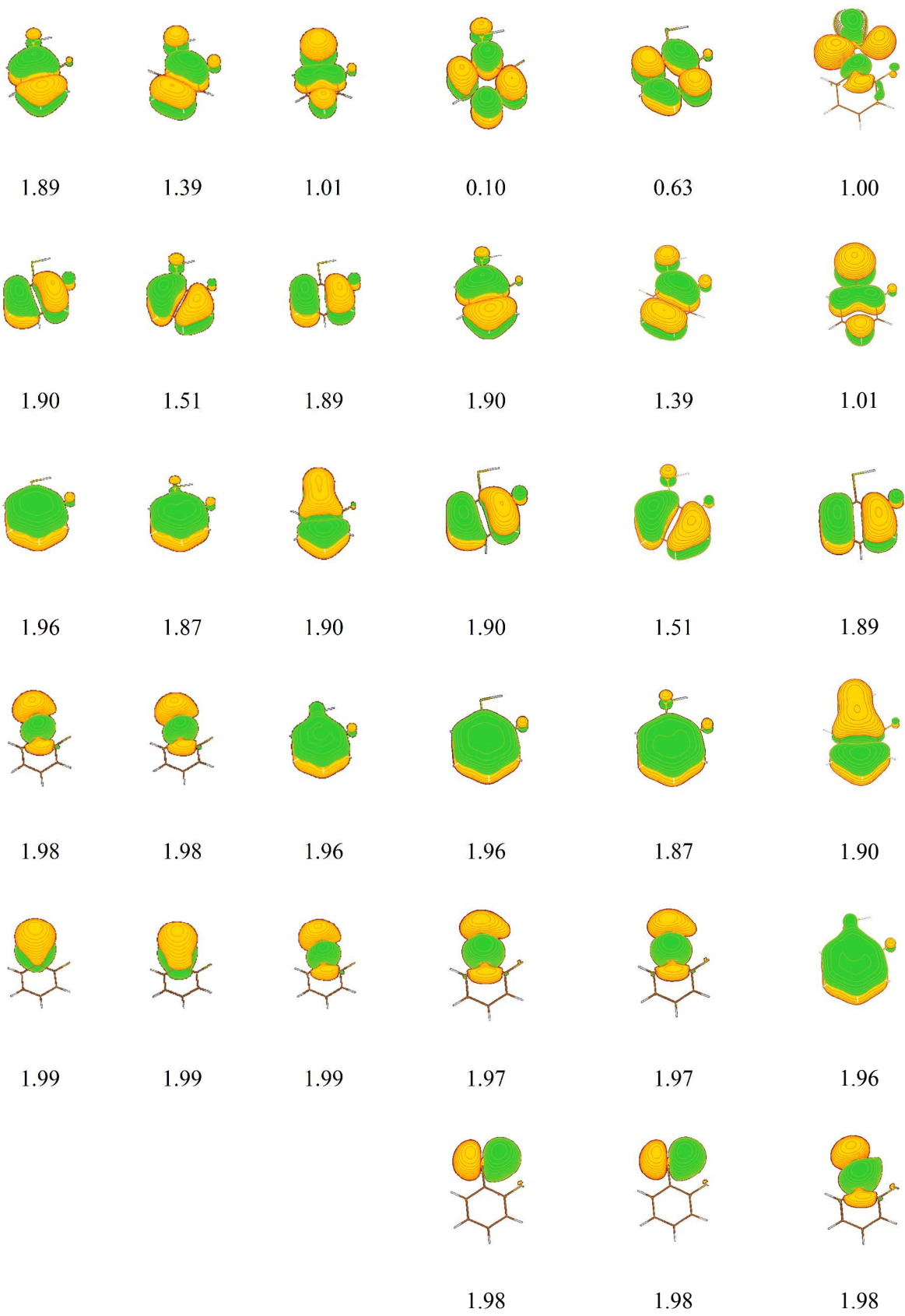
Table of Contents

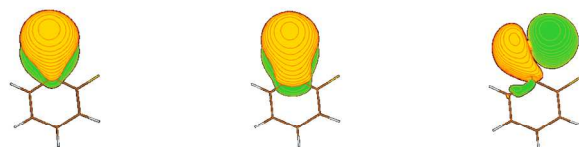
1. Molecular orbitals used for the CASSCF calculations
2. Cartesian axes of the molecular structure obtained by TD-HCTH calculation
3. R2PI and Franck-Condon simulation spectra
4. SEVI spectroscopy of 2-fluorothiophenol and 2-chlorothiophenol
5. Potential energy curves along CSH(D) dihedral angle
6. Fitting of total translational energy distributions and determination of \tilde{X}/\tilde{A} branching ratios
7. The calculation of energy gaps between \tilde{X} and \tilde{A} states of 2-fluorophenylthiyl and 2-chlorophenylthiyl radicals
8. Total translational energy distributions for the dissociation of 2-fluorothiophenol-d₁

1. Molecular orbitals used for the CASSCF calculations

Table S1. Molecular orbital (MO) diagrams and associated occupation numbers (Occ.) of three relevant neutral electronic states (S_0 , S_1 , S_2) of 2-fluorothiophenol at the S_0 equilibrium structure, which were obtained at SA3-CASSCF/6-311++G(3df,3pd) level of calculation where the active space of CAS(10,9) and CAS(12,11) was in the three columns from the left and in the remain columns, respectively.

State	S_0	S_1	S_2	S_0	S_1	S_2
MO						
Occ.	0.02	0.02	0.04	0.02	0.02	0.03
						
	0.04	0.11	0.10	0.03	0.03	0.04
						
	0.10	0.50	0.11	0.04	0.11	0.10
						
	0.10	0.63	1.01	0.10	0.50	0.11





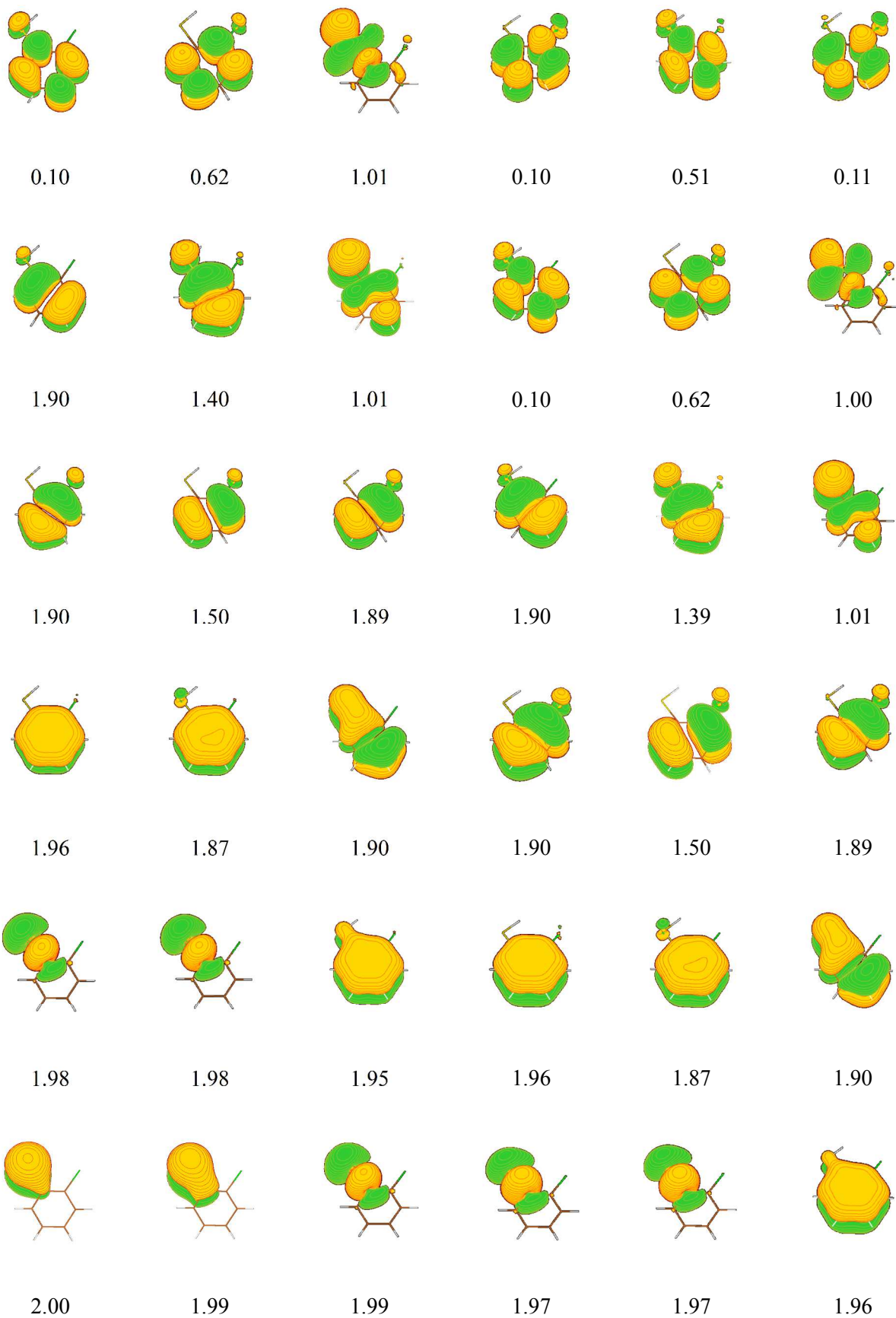
1.99

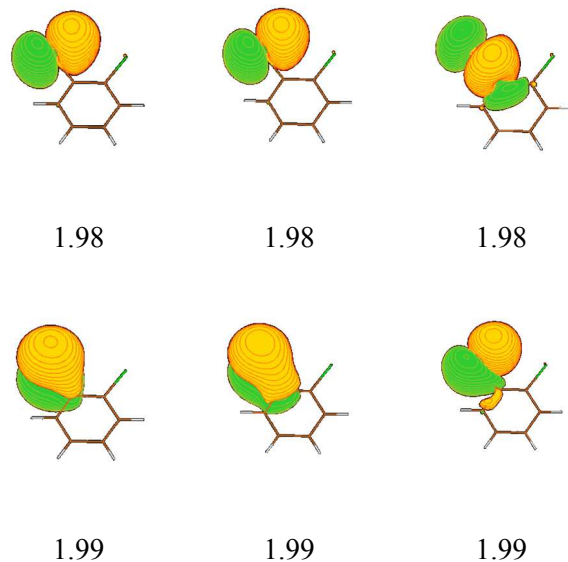
1.99

1.99

Table S2. Molecular orbital (MO) diagrams and associated occupation numbers (Occ.) of three relevant neutral electronic states (S_0 , S_1 , S_2) of 2-chlorothiophenol at the S_0 equilibrium structure, which were obtained at SA3-CASSCF/6-311++G(3df,3pd) level of calculation where the active space of CAS(10,9) and CAS(12,11) was in the three columns from the left and in the remain columns, respectively.

State	S_0	S_1	S_2	S_0	S_1	S_2
MO						
Occ.	0.02	0.02	0.04	0.02	0.02	0.03
	0.04	0.11	0.11	0.03	0.03	0.04
	0.10	0.52	0.11	0.04	0.11	0.11





2. Cartesian axes of the molecular structure obtained by TD-HCTH calculation

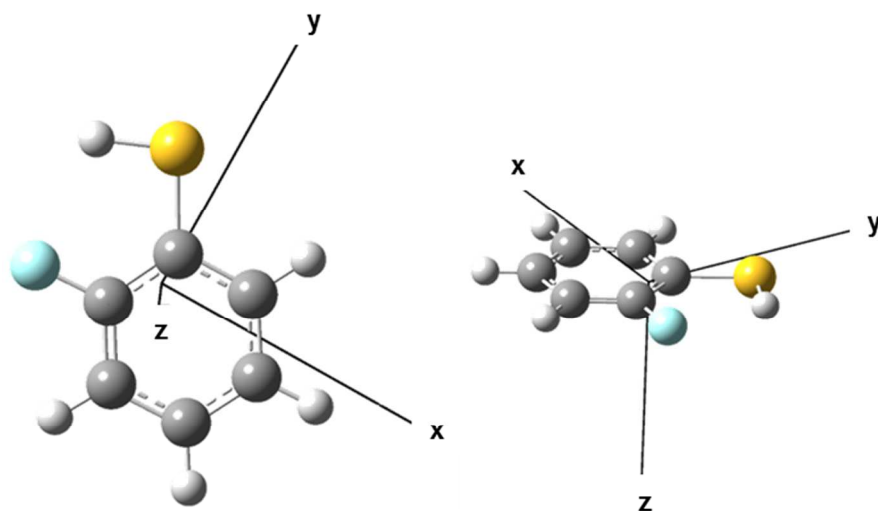


Figure S1. The Cartesian axes of the molecular structure obtained at TD-HCTH/6-311++G(3df,3pd) level of calculation, which is corresponding to both 2-fluorothiophenol and 2-chlorothiophenol.

3. R2PI and Franck-Condon simulation spectra

The minimum energy structures and vibrational frequencies for the S_0 and S_1 states of 2-fluorothiophenol and 2-chlorothiophenol were obtained by using (TD)-B3LYP/6-311++G(3df,3pd) level of calculation. Based on this, the Franck-Condon analysis was carried out using the Duschinsky transformation with a code developed by Peluso and coworkers.^{1,2}

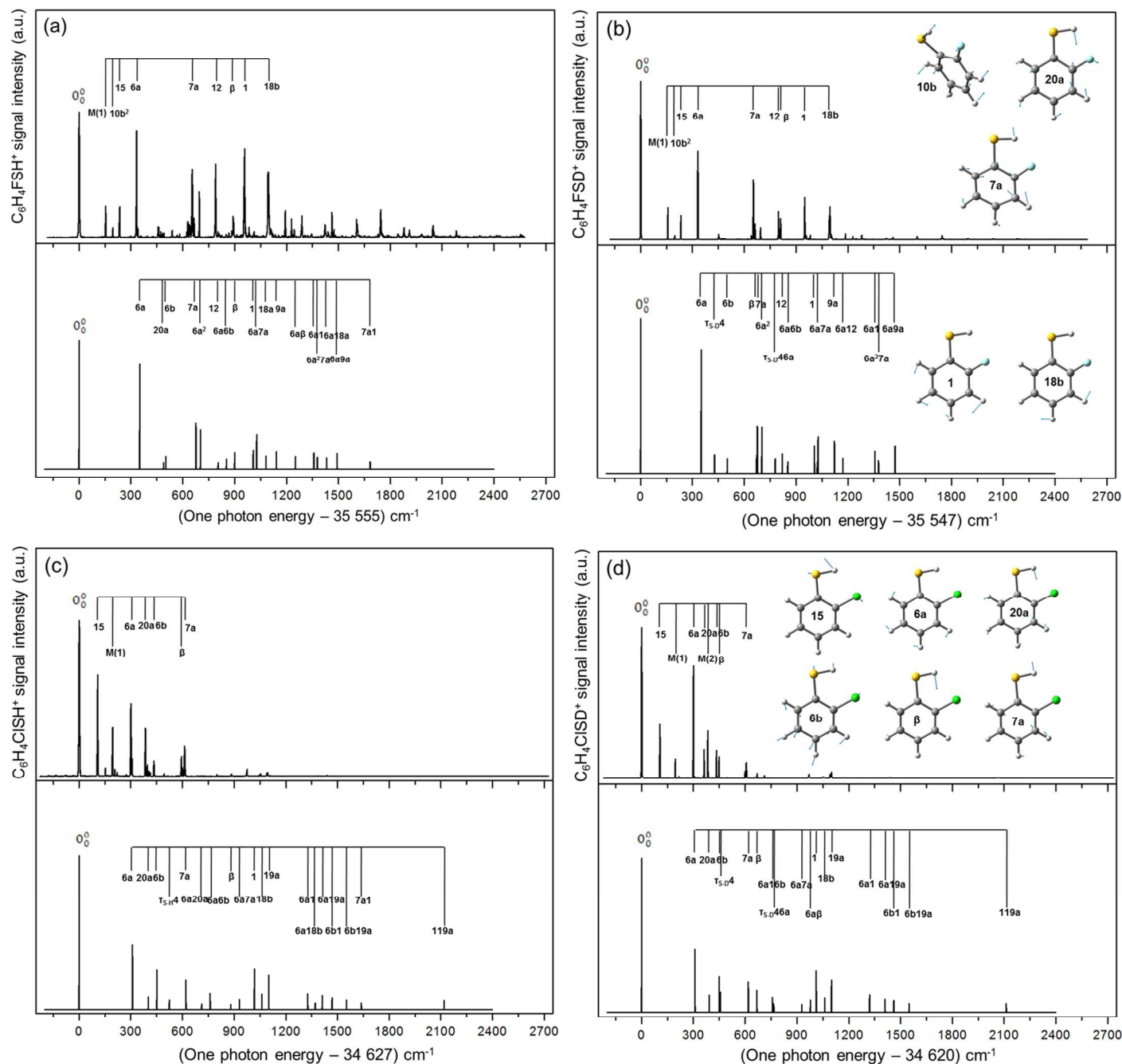


Figure S2. R2PI spectra (upper) of 2-fluorothiophenol(-d₁) (a-b) and 2-chlorothiophenol(-d₁) (c-d) with the corresponding Franck-Condon simulation spectra (lower). Some of vibrational modes are indicated in the inset.

Table S3. (TD)-B3LYP/6-311++G(3df,3pd) level calculated vibrational frequencies (cm^{-1}) of 2-fluorothiophenol(-d₁). The values in parentheses were obtained from experiment.

2-fluorothiophenol-h ₁					2-fluorothiophenol-d ₁				
Mode ^a	Symmetry	S ₀ ^b	S ₁ ^b	D ₀	Mode ^a	Symmetry	S ₀ ^b	S ₁ ^b	D ₀
$\tau_{\text{S-H}}$	a''	185	175	388	$\tau_{\text{S-H}}$	a''	128	146	289
10b	a''	149	128	130 (125)	10b	a''	155	124	128 (125)
15	a'	235	231 (235)	245 (245)	15	a'	230	225 (233)	239 (241)
4	a''	272	309	253	4	a''	270	282	252
6a	a'	371	351 (333)	374 (375)	6a	a'	371	351 (332)	374 (373)
16b	a''	453	369	437	16b	a''	453	368	433
20a	a'	496	489 (457)	496 (486)	20a	a'	486	478 (451)	488 (482)
16a	a''	550	584	497	16a	a''	549	584	489
6b	a'	559	501	541	6b	a'	558	501	540
7a	a'	688	676 (655)	690 (682)	7a	a'	687	676 (654)	690 (678)
					β	a'	695	672 (811)	702 (899)
17b	a''	724	454	717	17b	a''	724	454	717
11	a''	769	739	788	11	a''	769	739	787
12	a'	826	804 (790)	830 (821)	12	a'	834	820 (799)	840 (848)
10a	a''	874	407	897	10a	a''	874	397	897
17a	a''	961	159i ^c	998	17a	a''	961	158i ^c	998
β	a'	937	900 (892)	942 (925)					
5	a''	994	914	1022	5	a''	994	914	1022
1	a'	1055	1007 (957)	1025 (1007)	1	a'	1054	1006 (951)	1024 (1008)
18a	a'	1099	1081	1128	18a	a'	1095	1078	1123
18b	a'	1146	1044 (1095)	1158 (1142)	18b	a'	1144	1043 (1097)	1157 (1143)
9b	a'	1184	1176	1198	9b	a'	1184	1176	1194
9a	a'	1242	1141	1251	9a	a'	1240	1122	1244
3	a'	1291	1399	1313	3	a'	1289	1399	1312
14	a'	1327	1367	1363	14	a'	1325	1367	1361
19b	a'	1474	1440	1454	19b	a'	1473	1440	1453
19a	a'	1511	1536	1466	19a	a'	1511	1535	1465
8b	a'	1613	1494	1539	8b	a'	1612	1493	1539

8a	a'	1635	1536	1626	8a	a'	1634	1535	1625
$\nu_{\text{S-H str.}}$	a'	2709	2669	2650	$\nu_{\text{S-H str.}}$	a'	1945	1916	1903
7b	a'	3176	3173	3197	7b	a'	3176	3173	3197
13	a'	3187	3196	3202	13	a'	3187	3196	3202
20b	a'	3198	3231	3216	20b	a'	3198	3231	3216
2	a'	3208	3249	3220	2	a'	3208	3249	3220

[a] Normal modes were labeled according to Ref. 3.

[b] Vibrational frequencies were used for Franck-Condon simulation.

[c] An imaginary frequency which has little to do with reaction coordinate was excluded for Franck-Condon simulation.

Table S4. (TD)-B3LYP/6-311++G(3df,3pd) level calculated vibrational frequencies (cm^{-1}) of 2-chlorothiophenol(-d₁). The values in parentheses were obtained from experiment.

2-chlorothiophenol-h ₁					2-chlorothiophenol-d ₁				
Mode ^a	Symmetry	S ₀ ^b	S ₁ ^b	D ₀	Mode ^a	Symmetry	S ₀ ^b	S ₁ ^b	D ₀
$\tau_{\text{S-H}}$	a''	155	200	385 (380)	$\tau_{\text{S-H}}$	a''	112	155	290
10b	a''	132	95	106 (106)	10b	a''	133	95	104
15	a'	219	220 (108)	227 (213)	15	a'	215	215 (107)	222
4	a''	240	323	223	4	a''	236	302	222
6a	a'	327	310 (301)	326 (325)	6a	a'	326	309 (301)	326
16b	a''	449	428	478	16b	a''	449	428	466
20a	a'	419	402 (385)	412 (409)	20a	a'	409	392 (362)	402
16a	a''	524	399	438	16a	a''	524	399	435
6b	a'	472	451 (435)	489 (485)	6b	a'	472	449 (434)	488
7a	a'	668	620 (613)	650 (637)	7a	a'	665	618 (607)	645
					β	a'	687	668 (449)	688
17b	a''	718	597	700	17b	a''	718	596	700
11	a''	766	693	787	11	a''	766	693	786
12	a'	742	747	756 (759)	12	a'	752	754	766
10a	a''	878	534	896	10a	a''	878	533	896
17a	a''	970	134i ^c	1003	17a	a''	970	133i ^c	1003
β	a'	924	881 (594)	915 (908)					
5	a''	999	914	1025	5	a''	999	913	1025
1	a'	1061	1017	1034	1	a'	1059	1011	1033
18a	a'	1032	1028	1058	18a	a'	1029	1026	1050
18b	a'	1154	1061	1172 (1174)	18b	a'	1152	1061	1170
9b	a'	1188	1142	1194	9b	a'	1188	1130	1191
9a	a'	1491	1422	1452	9a	a'	1490	1422	1452
3	a'	1286	1194	1270	3	a'	1283	1191	1266
14	a'	1307	1337	1336	14	a'	1306	1335	1333
19b	a'	1456	1387	1430	19b	a'	1456	1387	1429
19a	a'	1134	1101	1135	19a	a'	1134	1100	1135

8b	a'	1596	1504	1525	8b	a'	1595	1504	1525
8a	a'	1618	1460	1608	8a	a'	1618	1459	1608
v _{S-H str.}	a'	2698	2640	2622	v _{S-H str.}	a'	1937	1895	1883
7b	a'	3173	3202	3194	7b	a'	3173	3202	3194
13	a'	3185	3169	3200	13	a'	3185	3169	3200
20b	a'	3197	3220	3216	20b	a'	3197	3220	3216
2	a'	3208	3242	3219	2	a'	3208	3242	3219

[a] Normal modes were labeled according to Ref. 3.

[b] Vibrational frequencies were used for Franck-Condon simulation.

[c] An imaginary frequency which has little to do with reaction coordinate was excluded for Franck-Condon simulation.

4. SEVI spectroscopy of 2-fluorothiophenol and 2-chlorothiophenol

According to Franck-Condon principle, the S_1 vibronic band is used as optical ladder or intermediate state in the stepwise (1+1') two-photon ionization process of slow electron velocity imaging (SEVI) experiments^{4,5}. Most cationic vibrational bands appeared in SEVI spectra follow propensity rule of $\Delta v = 0$ where the v is the quantum number of vibrational modes, and then S_1 vibrational bands can be inversely assigned when the ones of D_0 state are easily revealed by using ab initio calculation as the state is bound and has well-defined vibronic states. The SEVI spectra obtained via S_1 origin band excitation show quite strong origin bands to give ionization energy(IE) of $68375 \pm 20 \text{ cm}^{-1}$ for 2-fluorothiophenol(Fig. S3) and $68022 \pm 20 \text{ cm}^{-1}$ for 2-chlorothiophenol(Fig. S4). This indicates that the structural changes between S_1 origin and D_0 equilibrium are little, thus *cis* forms with a plane of symmetry are expected at S_1 origin bands when the minimum energy structures of D_0 states are also planar *cis* conformer revealed by DFT calculations for both substituted thiophenols. Angular momentum distributions of departed electrons in all SEVI spectra are parallel to the polarization of excitation laser, which implies that the electron is originated from the p shaped orbital indicating $\pi\pi^*$ nature of S_1 state. The vibrational bands appeared in the SEVI spectra were assigned with the basis of DFT calculation (Table S3 and Table S4). Then from this, the distinct vibronic bands in S_1 state could be assigned in Table S5 and Table S6.

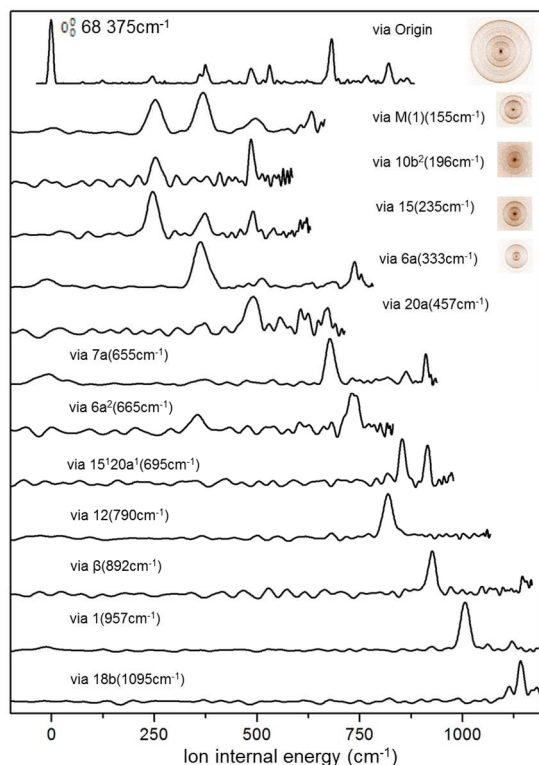


Figure S3. SEVI spectra of 2-fluorothiophenol with the several S_1 intermediate vibronic bands indicated in each figure. See Table S3 for the assignment.

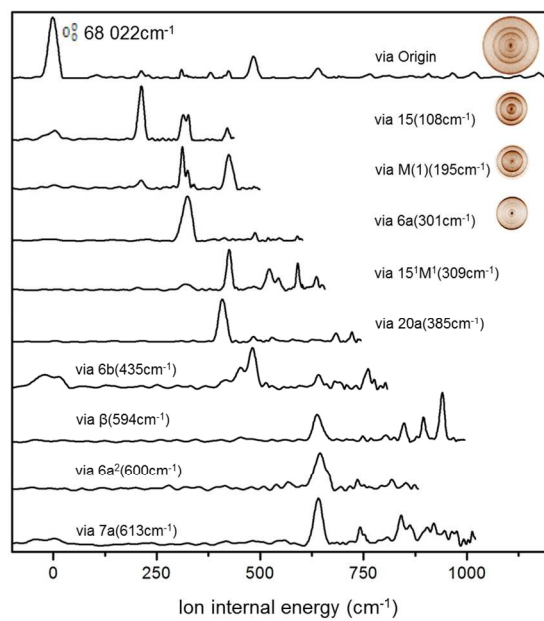


Figure S4. SEVI spectra of 2-chlorothiophenol with the several S_1 intermediate vibronic bands indicated in each figure. See Table S4 for the assignment.

Table S5. Assignment of S₁ vibronic bands of 2-fluorothiophenol(-d₁) based on the Franck-Condon simulation and SEVI spectra.

2-fluorothiophenol-h ₁			2-fluorothiophenol-d ₁		
Energy ^a (cm ⁻¹)	S ₁ internal energy ^a (cm ⁻¹)	Assignment ^b	Energy ^a (cm ⁻¹)	S ₁ internal energy ^a (cm ⁻¹)	Assignment
35 555	0	0 ₀ ⁰	35 547	0	0 ₀ ⁰
35 710	155	M(1) ^c	35 705	158	M(1) ^c
35 751	196	10b ²	35 745	197	10b ²
35 790	235	15	35 780	233	15
35 888	333	6a	35 879	332	6a
36 012	457	20a ¹	35 998	451	20a ¹
36 210	655	7a	36 200	654	7a
36 220	665	6a ²	36 210	664	6a ²
36 250	695	15 ¹ 20a ¹	36 240	694	15 ¹ 20a ¹
36 345	790	12	36 346	799	12
			36 358	811	β
36 447	892	β			
36 512	957	1	36 498	951	1
36 650	1095	18b	36 644	1097	18b

[a] Major peaks appeared in R2PI spectra.

[b] Assignments were performed with the basis of SEVI spectra.

[c] Tentative assignment is given but the character of vibrational modes is same with 10b.

Table S6. Assignment of S₁ vibronic bands of 2-chlorothiophenol(-d₁) based on the Franck-Condon simulation and SEVI spectra.

2-chlorothiophenol-h ₁			2-chlorothiophenol-d ₁		
Energy ^a (cm ⁻¹)	S ₁ internal energy ^a (cm ⁻¹)	Assignment ^b	Energy ^a (cm ⁻¹)	S ₁ internal energy ^a (cm ⁻¹)	Assignment ^d
34 627	0	0 ₀ ⁰	34 620	0	0 ₀ ⁰
34 735	108	15	34 727	107	15
34 822	195	M(1) ^c	34 816	196	M(1) ^c
34 928	301	6a	34 921	301	6a
34 936	309	15 ¹ M(1) ¹	34 928	308	15 ¹ M(1) ¹
35 012	385	20a	34 982	362	20a
			35 003	383	M(2) ^e
35 062	435	6b	35 054	434	6b
			35 069	449	β
35 221	594	β			
35 227	600	6a ²	35 220	600	6a ²
35 240	613	7a	35 227	607	7a

[a] Major peaks appeared in R2PI spectra.

[b] Assignments were performed with the basis of SEVI spectra.

[c] Tentative assignment is given but the character of vibrational modes is same with 10b.

[d] Assignments were performed with the basis of 2-chlorothiophenol-h₁'s assignments.

[e] Tentative assignment is given. There is no corresponding peak for 2-chlorothiophenol-h₁ with this peak.

5. Potential energy curves along CCSH(D) dihedral angle

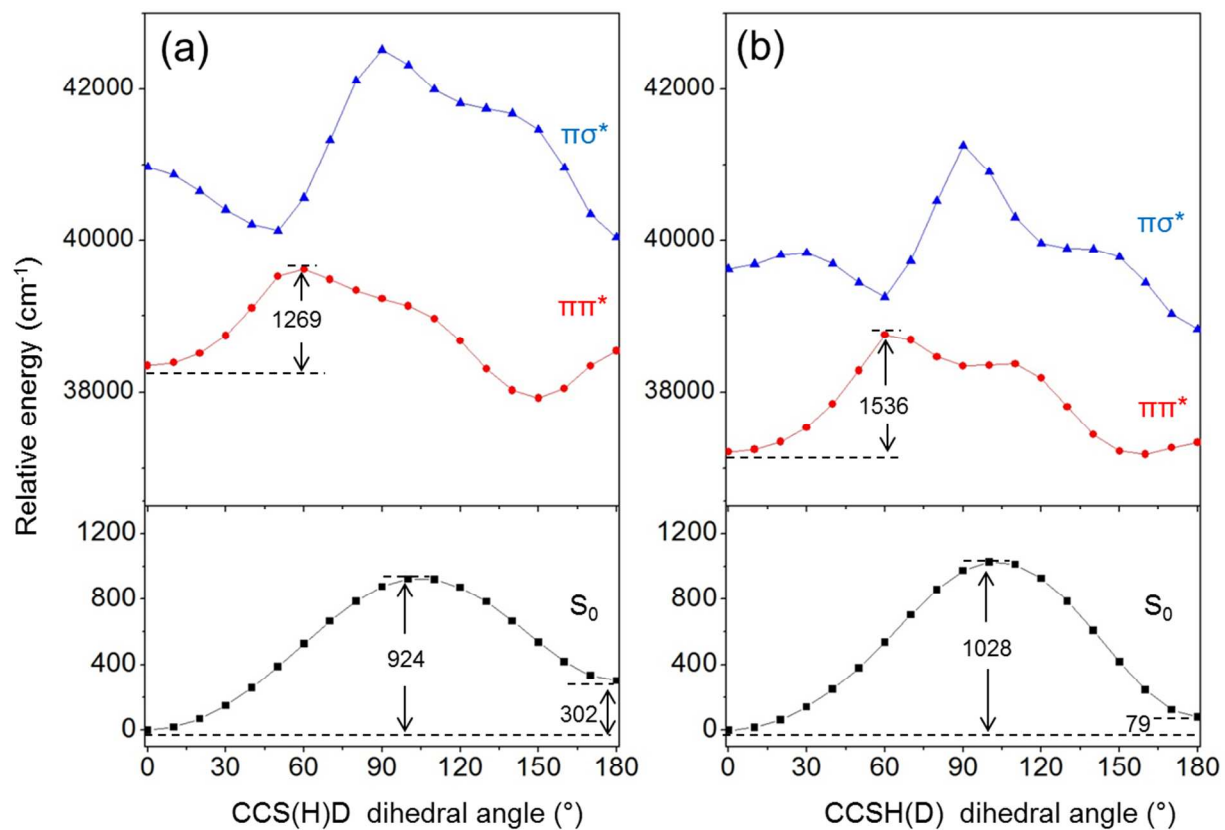


Figure S5. The PECs along CCSH(D) dihedral angle were calculated for the 2-fluorothiophenol(-d₁)(a) and 2-chlorothiophenol(-d₁)(b) by using (TD)-B3LYP/6-311++G(3df,3pd) level of calculation. The molecular structures of S₀ state are fully optimized at the specific dihedral angle.

6. Fitting of total translational energy distributions and determination of \tilde{X}/\tilde{A} branching ratios

The total translational energy distributions were fitted with the sum of two Boltzmann-like statistical functions, two Gaussian functions and the signals contributed from the probe laser only, which are given in Figure 3 and 4. Firstly, two Boltzmann-like functions were used to fit the broad background covering from lower to higher translational energy distributions:

$$P_{Background}(E) = A(1)\sqrt{E}\left(\frac{1}{B(1)}\right)^{\frac{3}{2}}e^{\left(\frac{-E}{B(1)}\right)} + A(2)\sqrt{E}\left(\frac{1}{B(2)}\right)^{3/2}e^{\left(\frac{-E}{B(2)}\right)} \quad (\text{Equation 1})$$

where the E was the total translational energy, $A(1)$ was the amplitude of the first Boltzmann-like function to fit the lower part of background signal while $B(1)$ was the width of that function. The parameters of $A(2)$ and $B(2)$ were used for second Boltzmann-like function to fit with the higher energy part of background. Then, two Gaussian functions were used to fit with real signal to give the \tilde{X}/\tilde{A} branching ratios:

$$P_{real\ signal}(E) = a(1)e^{\left(-\frac{2(E-b(1))^2}{c(1)^2}\right)} + a(2)e^{\left(-\frac{2(E-b(2))^2}{c(2)^2}\right)} \quad (\text{Equation 2})$$

where E was the total translational energy, the values of $a(1)$, $b(1)$, $c(1)$ were found out to fit with the \tilde{A} state of the product while $a(2)$, $b(2)$ and $c(2)$ were used for the \tilde{X} state at higher translational energy. To determine the error range for the \tilde{X}/\tilde{A} branching ratios, we obtained several ion images at a specific S_1 vibrational excitations. However, the uncertainty of the branching ratio induced from the Boltzmann-like fitting cannot be neglected. The translational energy distributions were, therefore, again fitted without the Boltzmann-like function to give the maximum error range for the \tilde{X}/\tilde{A} branching ratios (Fig. S6). This covers the error induced from the several images obtained at the same S_1 excitation energy.

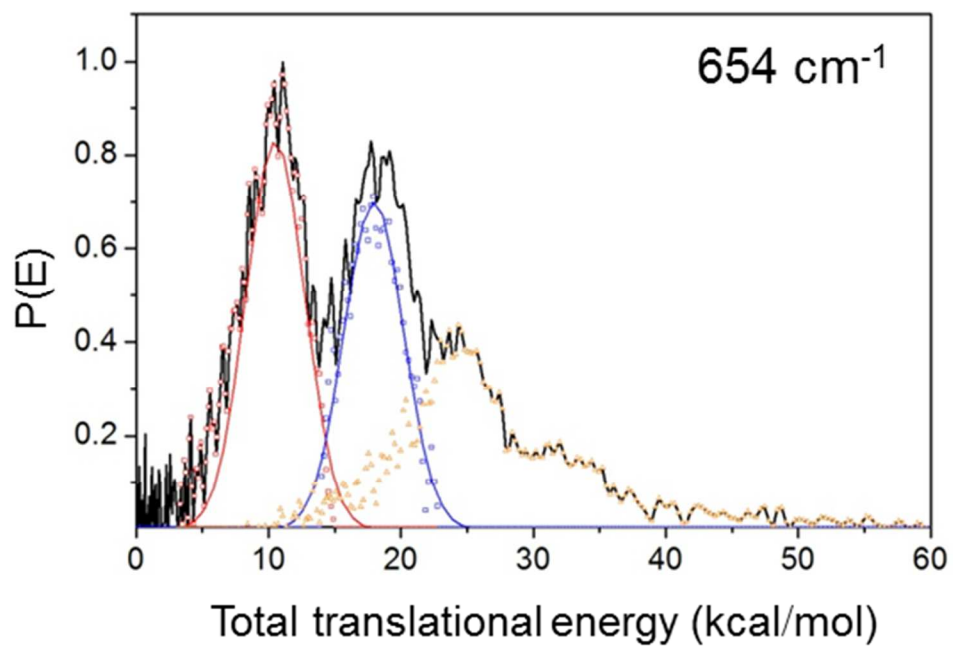
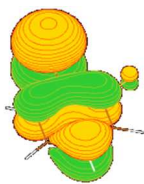
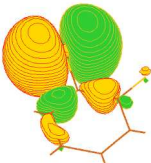


Figure S6. Total translational energy distributions fitted with two Gaussian functions (red and blue lines) and contributions from probe laser only (Orange triangles) but without the Boltzmann-like function.

7. The calculation of energy gaps between \tilde{X} and \tilde{A} states of 2-fluoro(chloro)phenylthiyl radicals

Table S7. Total energies of singly occupied molecular orbitals (SOMOs) and adiabatic excitation energies for the \tilde{X}^2A'' and \tilde{A}^2A' electronic states of the 2-fluorophenylthiyl radical calculated at the B3LYP, CASSCF and CASPT2 levels. The values in parentheses are for the 2-chlorophenylthiyl radical and inset figures represent SOMO of 2-fluorophenylthiyl radical.

Basis set	Total energies of SOMO (hartree)		$\tilde{A}^2A' \leftarrow \tilde{X}^2A''$ excitation energies (cm ⁻¹)
	X^2A''	A^2A' (adiabatic)	Adiabatic
<div style="display: flex; justify-content: space-around; align-items: center;">   </div>			
B3LYP			
6-311++g(3df,3pd)	-729.19042184	-729.17695530	2955.6
	(-1089.541738)	(-1089.5314284)	(2262.6)
cc-pVTZ	-729.19724391	-729.18393012	2922.1
	(-1089.55161505)	(-1089.54167649)	(2181.3)
CASSCF(9,8)			
6-311++g(3df,3pd)	-726.67233342	-726.66278909	2094.7
	(-1086.7104966)	(-1086.70304235)	(1636.0)
cc-pVTZ	-726.68265395	-726.67334753	2042.5
	(-1086.72495919)	(-1086.71793176)	(1542.3)
CASPT2			
6-311++g(3df,3pd)	-727.94955824	-727.93627556	2915.2
	(-1087.93046130)	(-1087.92002669)	(2290.1)
cc-pVTZ	-727.95162714	-727.93908928	2751.7
	(-1087.93908535)	(-1087.92929937)	(2147.8)

8. Total translational energy distributions for the dissociation of 2-fluorothiophenol-d₁

The total translational energy distributions of 2-fluorothiophenol-d₁ were obtained at higher excitation energies. Namely, within the internal energies up to ~ 6900 cm⁻¹ above the S₁ origin band, there are no R2PI signal and ion images of D atom fragments becomes anisotropic, indicating quite fast dissociation (Fig. S7(c)). Moreover, below ~ 3200 cm⁻¹ of internal energy, the peak for the \tilde{A} state of C₆H₄FS· quite slightly increases compared to the increase of the excitation energy but drastically increase above this energy, which implies that the portion of S₂ state is dominant just above this energy (Fig. S7(a)-(b)).

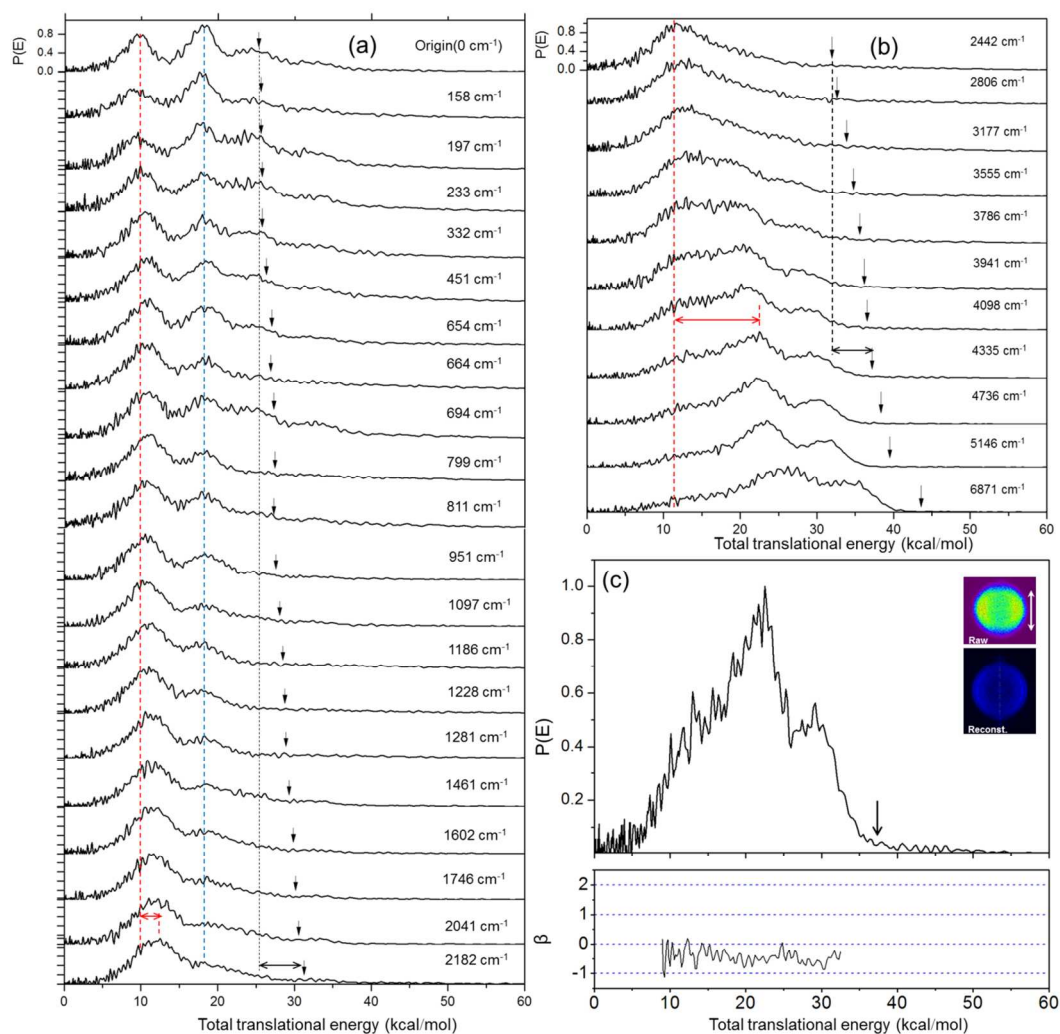


Figure S7. Total translational energy distributions (a-b) of 2-fluorothiophenol-d₁ obtained at several excitation energies up to ~ 6900 cm⁻¹ above the S₁ origin band, which are indicated in each figure. The magnified one obtained at excitation energy of 4335 cm⁻¹ is given in (c). The black arrows represent the maximum available energy when the lower limit of S-D bond dissociation energy is given as 26874 cm⁻¹ which is the energy difference between S₁ origin excitation energy and maximum translational energy of the \tilde{X} state. Blue, Red and black dashed lines positioned at the peaks of \tilde{X} , \tilde{A} states, and maximum available energy at S₁ origin are used for the visual guide.

REFERENCES

- (1) Borrelli, R.; Peluso, A. Dynamics of Radiationless Transitions in Large Molecular Systems: A Franck–Condon-based Method Accounting for Displacements and Rotations of all the Normal Coordinates. *J. Chem. Phys.* **2003**, *119*, 8437–8448.
- (2) Peluso, A.; Santoro, F.; Rinte, G. D. Vibronic Coupling in Electronic Transitions with Significant Duschinsky Effect. *Int. J. Quantum. Chem.* **1997**, *63*, 233–244.
- (3) G. Varsa'nyi, Ed. *Assignments for Vibrational Spectra of 700 Benzene Derivatives*; Wiley: New York, 1974.
- (4) Osterwalder, A.; Nee, M. J.; Zhou, J.; Neumark, D. M. High Resolution Photodetachment Spectroscopy of Negative Ions via Slow Photoelectron Imaging. *J. Chem. Phys.* **2004**, *121*, 6317–6322.
- (5) Neumark, D. M. Slow Electron Velocity-Map Imaging of Negative Ions: Applications to Spectroscopy and Dynamics. *J. Phys. Chem. A* **2008**, *112*, 13287–13301.
- (6) *PGOPHER, A Program for Simulating Rotational Structure*, Wester, C. M.; University of Bristol, <http://pgopher,chem.bris.ac.uk>.